ACS Photonics

Article

pubs.acs.org/journal/apchd5

Cavity-Photon Controlled Thermoelectric Transport through a Quantum Wire

Nzar Rauf Abdullah,*[,†,∥] Chi-Shung Tang,[‡] Andrei Manolescu,[§] and Vidar Gudmundsson*[,∥]

[†]Physics Department, Faculty of Science and Science Education, School of Science, University of Sulaimani, Kurdistan, Iraq

[∥]Science Institute, University of Iceland, Dunhaga 3, IS-107 Reykjavik, Iceland

[‡]Department of Mechanical Engineering, National United University, 2, Lienda, Miaoli 36063, Taiwan

[§]School of Science and Engineering, Reykjavik University, Menntavegur 1, IS-101 Reykjavik, Iceland

ABSTRACT: We investigate the influence of a quantized photon field on thermoelectric transport of electrons through a quantum wire embedded in a photon cavity. The quantum wire is connected to two electron reservoirs at different temperatures leading to the generation of a thermoelectric current. The transient thermoelectric current strongly depends on the photon energy and the number of photons initially in the cavity. Two different regimes are studied, off-resonant and on-resonant polarized fields, with photon energy smaller than, or equal to, the energy spacing between some of the lowest states in the quantum wire. We observe that the current is inverted for the off-resonant photon field due to participation of photon replica states in the transport. A reduction in the current is recorded for the resonant photon field, a direct consequence of the Rabi-splitting.

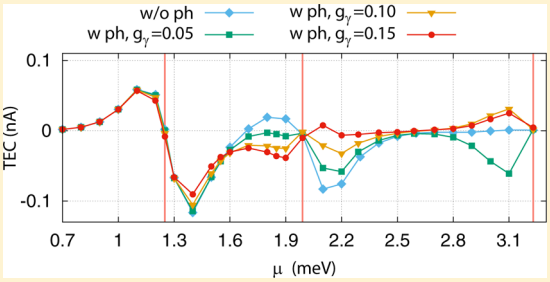

KEYWORDS: *cavity quantum electrodynamics, thermoelectric transport, quantum wire, quantum master equation*

Thermoelectric transport is a subject of intense study for future energy harvesting devices.[1,2] Low-dimensional electronic systems have a potential to improve thermoelectric efficiency compared to bulk electronic materials due to their highly peaked density of states for system sizes in the range of nanometers.[3] A thermoelectric current (TEC) can be generated by a temperature gradient ΔT in an electronic system. In the linear response regime, the temperature difference approaches zero and the thermoelectric efficiency is characterized by the dimensionless figure of merit ZT.[4] In the nonlinear response regime, the thermoelectric efficiency is represented by the bias voltage ΔV generated by ΔT.[5] In both regimes, the thermal efficiency can be high in nanodevices.

Since the 1990s, various aspects of thermoelectric transport have been investigated in several types of quantum systems, such as single quantum dots,[6−8] double quantum dots,[9−11] quantum wires,[12,13] or nanowires.[14] The Coulomb interaction between the charge carriers influences the thermal transport through small structures like quantum dots, forming plateaus (Coulomb blockade) in the TEC.[7,8,15] The transition from the Coulomb blockade regime to the Kondo regime in thermoelectric transport has been studied for a single-level quantum dot.[16,17] Dynamic aspects of thermoelectric transport have been investigated,[10,18] and the influence of static nonlinear behavior on the efficiency of power conversion has been studied.[19] In mesoscopic systems, the dephasing and inelastic scattering processes are found to affect the thermoelectric transport and generate a magnetic field asymmetry in the Seebeck coefficient.[20] The thermoelectric effect through a serial double quantum dot weakly coupled to ferromagnetic leads has been investigated, and the influence of temperature and interdot tunneling on the figure of merit has been demonstrated.[21] In the above-mentioned examples, the thermoelectric effect has been investigeted in the steady state regime. Recently, a method to study the time-dependent thermal transport in nanoscale devices has been proposed. The approach has been shown to recover the linear relation between the thermal current and the temperature gradient.[22]

Another interesting aspect of this issue is the importance of photon radiation to control thermal transport. Recently, time-dependent photon radiation has been used to enhance the heat and thermoelectric transport.[23,24] Photonic heat current through an arbitrary circuit element coupled to two dissipative reservoirs has been explored at finite temperatures.[25] Transfer of heat via photons between two metals is reported in a study of photonic thermopower, where the metals are coupled by a circuit containing a linear reactive impedance.[26]

An active field of research is the search for an appropriate thermodynamic description of mesoscopic electron systems. We will circumvent this issue here by using an approach commonly applied to small open systems, but the reader interested in the possibility to use linear response formalism we refer to a study of Balachandran et al.[27]

Here, we describe the TEC in a finite quantum wire (the central system) coupled to two leads (electron reservoirs) with different temperatures, but at the same chemical potential. The

Received: September 23, 2015
Published: January 19, 2016

DOI: 10.1021/acsphotonics.5b00532
ACS Photonics 2016, 3, 249−254

temperature gradient causes electron flow from the leads to the quantum wire and vice versa. In addition, the quantum wire is coupled to a cavity field with photons polarized in the direction of the electron propagation in the quantum wire. A generalized master equation formalism is used to calculate the time-dependent evolution of the electrons in the quantum wire.[28] We show how the TEC can be controlled by cavity parameters such as the photon energy in either off-resonant or resonant condition. The single photon mode in the cavity can change both the magnitude and the sign of the thermal current induced by the temperature gradient. Therefore, the use of cavity photons can be seen as a new method to amplify or control thermoelectric current in nanodevices.

MODEL

We assume a short GaAs quantum wire formed in a two-dimensional electron gas in the $x-y$ plane, with an effective mass $m^* = 0.067m_e$ and relative dielectric constant $\kappa = 12.3$. The quantum wire is hard-wall confined at the ends in the x-direction, the transport direction, and parabolically confined in the y-direction. The wire with length $L_x = 150$ nm is weakly coupled to two leads held at different temperatures. The total system is exposed to an external perpendicular static magnetic field $B = 0.1$ T with cyclotron energy $\hbar\omega_c = 0.172$ meV. The transverse confinement energy of the electrons in the quantum wire is equal to that of the leads $\hbar\Omega_0 = \hbar\Omega_l = 2.0$ meV, where l refers to the left (L) or the right (R) lead. The effective confinement frequency is $\Omega_\omega = \sqrt{\Omega_0^2 + \omega_c^2}$.

The many-body Hamiltonian of the coupled electron-photon system is

$$H = H_e + H_\gamma + H_{e-\gamma} \tag{1}$$

where H_e is the Hamiltonian of the electronic system, including the static Coulomb repulsion between the electrons[29]

$$H_e = \int dr\psi^\dagger(\mathbf{r})\left[\frac{\boldsymbol{\pi}^2}{2m^*} + \frac{1}{2}m^*\Omega_0^2 y^2\right]\psi(\mathbf{r}) + \int dr \int dr'\psi^\dagger(\mathbf{r})\psi^\dagger(\mathbf{r}')U_C(\mathbf{r},\mathbf{r}')\psi(\mathbf{r}')\psi(\mathbf{r}) \tag{2}$$

Herein, $\boldsymbol{\pi} = \mathbf{p} + (e/c)\mathbf{A}$, with $\mathbf{p}$ the canonical momentum, and $\mathbf{A} = -By\hat{\mathbf{x}}$ is the vector potential for the static external magnetic field $\mathbf{B} = B\hat{\mathbf{z}}$. $\psi(\mathbf{r}) = \sum_i \psi_i(r)d_i$ and $\psi^\dagger(\mathbf{r}) = \sum_i \psi_i^*(r)d_i^\dagger$ are the Fermionic field operators with $d_i(d^\dagger{}_i)$ being the annihilation-(creation) operators for an electron in the single electron state $|i\rangle$ corresponding to ψ_i. The second term of the eq 2 is the electron−electron interaction in the quantum wire with U_C being the Coulomb interaction potential.[30]

The cavity photon field is defined by the quantized vector potential $\mathbf{A}_\gamma$ in the Coulomb gauge. Therefore, the second term in the eq 1 can be written as $H_\gamma = \hbar\omega_\gamma a^\dagger a$ introducing the Hamiltonian of the single free cavity photon mode with energy $\hbar\omega_\gamma$, and $a(a^\dagger)$ being the photon annihilation(creation) operators. The vector potential of the photon field $\mathbf{A}_\gamma$ is given by $\mathbf{A}_\gamma(\mathbf{r}) = \mathcal{A}(a + a^\dagger)\mathbf{e}$, with $\mathcal{A}$ the amplitude of the photon field, and $\mathbf{e} = \mathbf{e}_x$ for parallel polarized photon field (TE_{011}), or $\mathbf{e} = \mathbf{e}_y$ for perpendicular polarized photon field (TE_{101}). We have assumed the wavelength of the cavity mode to be much larger than the size of the electron system, L_x. The last term of eq 1 represents the full electron−photon interaction

$$H_{e-\gamma} = -\frac{1}{c}\int d\mathbf{r}\mathbf{j}(\mathbf{r})\cdot\mathbf{A}_\gamma - \frac{e}{2m^*c^2}\int d\mathbf{r}\rho(\mathbf{r})A_\gamma^2 \tag{3}$$

including both the para- and the diamagnetic interactions, respectively.[30] The charge is $\rho = -e\psi^\dagger\psi$, and the charge current density is defined by

$$\mathbf{j} = -\frac{e}{2m^*}\{\psi^\dagger(\boldsymbol{\pi}\psi) + (\boldsymbol{\pi}^*\psi^\dagger)\psi\} \tag{4}$$

The electron−electron and the electron−photon interactions are treated by exact diagonalization in appropriately truncated Fock-spaces constructed from a tensor product of the eigenstates of the single-electron Hamiltonian, and the eigenstates of the photon number operator. The characteristic energy scale of the electron-photon coupling (effective coupling constant) is $g_\gamma = eAa_\omega\Omega_\omega/c$.[31]

In order to calculate the thermoelectric current, a non-equilibrium property, we use a projection formalism[32,33] leading to a generalized non-Markovian master equation describing the time evolution of the reduced density operator $\rho_S(t)$ of the open central system (eq 1; the interacting electrons and cavity photons) under the dissipative influenced of the external leads, weakly coupled to the system, acting as a reservoir of electrons and energy.[34] The lead system coupling strength corresponds to 0.5 meV.

The coupling of the leads and the system is described by a tunneling Hamiltonian, with a contact region extending approximately 16 nm in the transport direction (x-direction) into the lead and the central system from their interface and 30 nm along the interface.[34] This guarantees that the coupling of the sub-bands in the leads and the central system observes their parity like is seen in a Lippmann−Schwinger scattering formalism.[35] In addition, the coupling of individual states in the leads and the central system depends on their presence in the contact region.

We define the thermoelectric current (TEC), in the steady state, in terms of the reduced density operator such that

$$\mathrm{TEC} = I_L = I_R \tag{5}$$

where I_L is the current from the left lead to the quantum wire defined as

$$I_L(t) = \mathrm{Tr}[\dot{\rho}_S^L(t)Q] \tag{6}$$

and the current from the quantum wire to the right lead (I_R) is

$$I_R(t) = -\mathrm{Tr}[\dot{\rho}_S^R(t)Q] \tag{7}$$

with the charge operator $Q = eN$ expressed in terms of the electron number operator N. The partial density operators $\rho_S^{L,R}$ correspond to the coupling of the central system to the L and R leads, respectively, and is more explicitly calculated, see Moldoveanu et al.,[36] in the weak coupling regime. In a steady state, the right and left currents are of the same magnitude, $I_L = I_R$, but in the transient regime, their difference indicates the charging or discharging of the central system. The steady state is independent of the original number of photons and electrons in the system, but in the later transient regime that we are interested in here, around $t \approx 220$ ps, the currents still depend on the original photon and electron numbers.

The photons in the cavity are linearly polarized in the x-direction. In the short quantum wire with uniform shape in the transport direction, this polarization strengthens the photon effects on the transport. We tune the photon energy and the number of photons initially present in the cavity in order to

DOI: 10.1021/acsphotonics.5b00532
ACS Photonics 2016, 3, 249−254

explore how these initial conditions or parameters can be used to control the TEC in the quantum wire in the late transient regime.

Figure 1 shows a schematic diagram of the quantum wire (white color) coupled to the left lead (red color) with

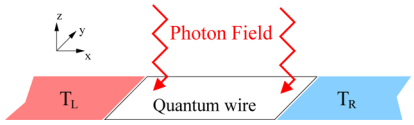

Figure 1. Schematic diagram of a quantum wire (white color) connected to a left lead (pink color) with temperature T_L and a right lead (blue color) with temperature T_R. The photon field is represented by the red zigzag arrows.

temperature T_L and the right lead (blue color) with temperature T_R. The red zigzag arrows indicate the polarized photon field.

OFF-RESONANCE PHOTON FIELD

In this section, we assume the photon energy is smaller than the energy spacing between the three lowest energy states of the quantum wire. For instance, the photon energy is $\hbar\omega_\gamma < E_1 - E_0$, where $E_0(E_1)$ is the energy of the ground state (first excited state) of the quantum wire, respectively.

Figure 2a shows the energy spectrum versus electron−photon coupling strength g_γ, where 0ES (golden circles) are

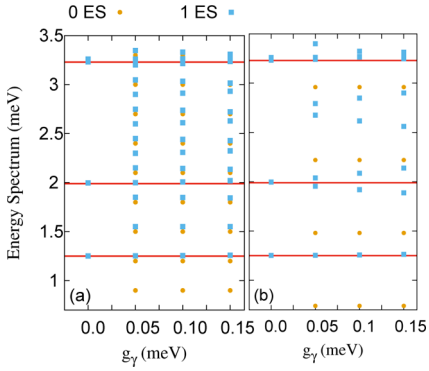

Figure 2. Energy spectrum of the quantum wire versus electron−photon coupling strength g_γ. 0ES (golden circles) are zero-electron states, 1ES (blue squares) are one-electron states, and the horizontal lines (red lines) display the location of the resonances of the leads with the three lowest one-electron states in the case of off-resonance (a) and resonance (b) photon field. The photon number is $N_\gamma = 2$, and the photons are linearly polarized in the x-direction. The magnetic field is $B = 0.1$ T, and $\hbar\Omega_0 = 2.0$ meV.

zero-electron states, 1ES (blue squares) are one-electron states, and the horizontal lines (red lines) indicate the location of the resonance condition for the lowest three one-electron states with the chemical potentials of the leads, $\mu_L = \mu_R = E_\mu$, at $g_\gamma = 0$. We start with no electron−photon coupling, $g_\gamma = 0.0$ meV. In this case, we concentrate our attention on the three lowest states in a selected range of the energy spectrum: the ground state, the first excited state, and the second excited state, with energy values $E_0 = 1.25$ meV, $E_1 = 1.99$ meV, and $E_2 = 3.23$ meV, respectively. In the presence of an electron−photon coupling, with an off-resonant photon field, photon replicas of the above-mentioned three states are formed. The separation between the photon replica states is approximately equal to the photon energy for the selected values of the electron−photon coupling strength used here. The photon replicas play an important role in the thermoelectric transport.

Figure 3 demonstrates the TEC (a) and the occupation (b) for the three lowest states of the quantum wire in the case of no

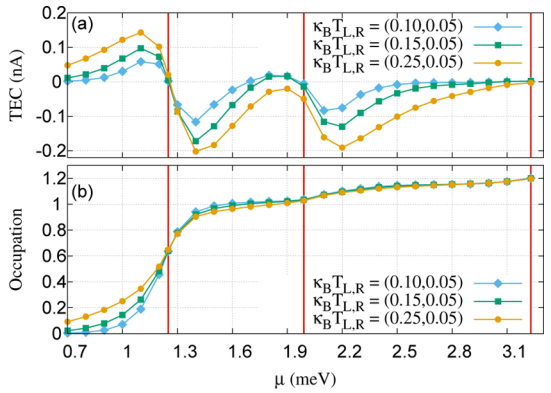

Figure 3. TEC (a) and occupation (b) as functions of the chemical potential $\mu = \mu_L = \mu_R$ plotted at time $t = 220$ ps. The temperature of the right lead is fixed at $T_R = 0.58$ K, implying thermal energy 0.05 meV, and varying the temperature of the left lead to $T_L = 1.16$, 1.742, and 2.901 K, implying thermal energies 0.1 (blue diamonds), 0.15 (green squares), and 0.25 meV (golden circles), respectively. The red vertical lines show the resonance condition for the ground state at $\mu = 1.25$ meV, the first excited state at $\mu = 1.99$ meV, and the second excited state at $\mu = 3.23$ meV, respectively. The magnetic field is $B = 0.1$ T, and $\hbar\Omega_0 = 2.0$ meV.

electron−photon coupling, $g_\gamma = 0.0$ meV. We fix the temperature of the right lead at $k_B T_R = 0.05$ meV, and vary the temperature of the left lead to $k_B T_L = 0.1$ (blue diamonds), 0.15 (green squares), and 0.25 meV (golden circles). In Figure 3a, the TEC as a function of chemical potential $\mu = \mu_L = \mu_R$ is plotted at time $t = 220$ ps. At this time point, the system is in the late transient regime very close to a steady state. The concept of a TEC can be loosely explained as being related to the Fermi functions of the leads. The TEC is zero in the following cases: half filling, where the Fermi function of the leads is equal to 0.5, and integer filling, where the Fermi function of the leads is either 0 or 1.[6]

For instance, the TEC is zero at $\mu = 1.25$ meV corresponding to approximately half filling of the ground state, as is shown in Figure 3b. In addition, the TEC is again zero at $\mu = 0.7$ and 1.7 meV for the integer filling of occupation 0 and 1, respectively.

In the presence of a higher temperature of the left lead at $k_B T_L = 0.25$ meV, a shifting in the TEC is observed for the first excited state at $\mu = 1.99$ meV. The current deviation occurs due to an increased thermal smearing at the higher temperature. In this case, both the ground state and the first excited state participate in the electron transport at $\mu = 1.99$ meV. Therefore, the current becomes negative, instead of the zero value at a lower temperature.

Furthermore, we notice that the second excited state of the quantum wire is in resonance with the second subband of the leads. The wave function of the second excited state of the central system is symmetric in the y-direction, while the wave functions of the second subband of the leads are antisymmetric in the y-direction. The electron transport from a symmetric to an antisymmetric state or vice versa is not allowed due to the geometry sensitive function that describes the coupling between the quantum wire and the leads.[28,34] Therefore, a

DOI: 10.1021/acsphotonics.5b00532
ACS Photonics 2016, 3, 249−254

plateau in the TEC is formed for the second excited state around $\mu = 3.23$ meV.

Now, we assume the quantum wire is embedded in a photon cavity with a photon mode of energy $\hbar\omega_\gamma = 0.3$ meV, and the cavity initially contains two photons $N_\gamma = 2$. The photons are linearly polarized in the x-direction. The photon energy is smaller than the energy spacing between the ground state and the first excited state on one hand, and the first excited state and the second excited state on the other hand. This means that the system is off-resonant with respect to the photon field. The energy spectrum of the quantum wire embedded in the cavity with off-resonant photon field was shown in Figure 2a.

The TEC as a function of the chemical potential of the leads is displayed in Figure 4a for the system without a photon cavity

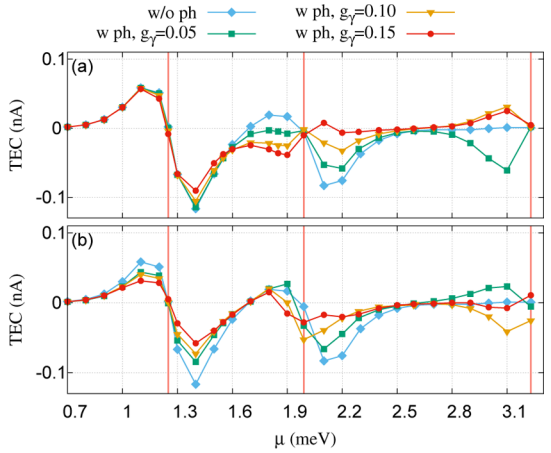

Figure 4. TEC as a function of the chemical potential $\mu = \mu_L = \mu_R$ plotted at time $t = 220$ ps without photon cavity $g_\gamma = 0.0$ meV (blue diamonds), and with photon cavity for the electron−photon coupling strength $g_\gamma = 0.05$ (green squares), 0.10 (golden triangles), and 0.15 meV (red circles) in the case of off-resonance (a) and resonance (b) photon field. The photons are linearly polarized in the x-direction. The temperature of the left (right) lead is fixed at $T_L = 1.16$ K ($T_R = 0.58$ K), implying thermal energy $k_BT_L = 0.10$ meV ($k_BT_R = 0.05$ meV). The magnetic field is $B = 0.1$ T, and $\hbar\Omega_0 = 2.0$ meV.

$g_\gamma = 0.0$ meV (blue diamonds) and with a photon cavity for the electron-photon coupling strength $g_\gamma = 0.05$ (green squares), 0.10 (golden triangles), and 0.15 meV (red circles) in the case of off-resonant photon field at time $t = 220$ ps. We observe that the current through the ground state is almost unchanged in the presence of a photon cavity, but the characteristics of the TEC of the first excited state and the second excited state are drastically modified. The influence of cavity photon field is to invert the TEC from "positive" to "negative" values or vice versa around the first excited state at $\mu = 1.99$ meV. The two-photon replica of the ground state at $\mu = 1.84$ meV contributes to the electron transport, with the first excited state leading to the current flip from "positive" to "negative" values. In addition, the two-photon replica of the first excited state around $\mu = 2.59$ meV becomes active in the transport. Therefore, the TEC is inverted from "negative" to "positive" values around $\mu = 2.1$ meV.

The electron transport is affected around the second excited state in the presence of the photon cavity, as is shown in Figure 4a. This is because the two-photon replica of the first excited state is getting into resonance with the second sub-band of the leads. The two-photon replica of the first excited state has an antisymmetric wave function in the y-direction, and the wave functions of the second sub-band are antisymmetric as well. Consequently, the electrons transfer from the second sub-band of the leads to the two-photon replica of the first excited state of the quantum wire. A TEC is thus generated.

The effects of the initial number of photons on the TEC is shown in Figure 5. The off-resonance system (Figure 5a) is

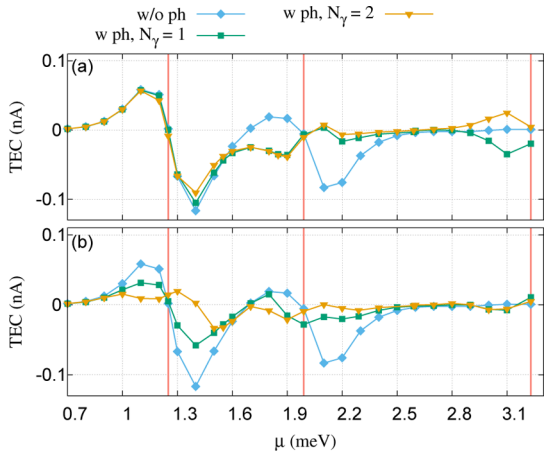

Figure 5. TEC as a function of the chemical potential $\mu = \mu_L = \mu_R$ plotted at time $t = 220$ ps without photon cavity $g_\gamma = 0.0$ meV (blue diamonds) and with photon cavity initially containing one photon, $N_\gamma = 1$ (green squares), and two photons, $N_\gamma = 2$ (golden triangles), in the case of off-resonance (a) and resonance (b) photon field. The photons are linearly polarized in the x-direction. The temperature of the left (right) lead is fixed at $T_L = 1.16$ K ($T_R = 0.58$ K), implying thermal energy $k_BT_L = 0.10$ meV ($k_BT_R = 0.05$ meV). The magnetic field is $B = 0.1$ T, and $\hbar\Omega_0 = 2.0$ meV.

rather insensitive to the exact number of photons in the low energy regime. This is because both one- and two-photon replica states are close to each other in the off-resonant photon field. The thermal smearing leads to participation of both states in the electron transport. Therefore, the selected initial photon number in the cavity does not influence the TEC.

ON-RESONANCE PHOTON FIELD

In this section we assume the photon energy is approximately equal to the energy spacing between the ground state and the first excited state, $\hbar\omega_\gamma \cong E_1 - E_0$. The system under consideration is in resonance with the photon field. The photon energy is assumed to be $\hbar\omega_\gamma = 0.74$ meV and the cavity initially contains one photon, $N_\gamma = 1$.

The energy spectrum of the quantum wire as a function of the electron-photon coupling strength g_γ in the presence of the resonant photon field is displayed in Figure 2b, where 0ES (golden circles) are zero-electron states and 1ES (blue squares) are one-electron states. The horizontal lines (red lines) display the energy of possible transport resonances. In the case of no electron−photon coupling at $g_\gamma = 0.0$ meV, the three states mentioned in the previous section are again found in the selected range of energy. In the presence of the cavity field, the one-photon replica of the ground state is observed near the first excited state at $g_\gamma = 0.05$ meV.

Increasing the electron−photon coupling strength to $g_\gamma = 0.15$ meV, the one-photon replica of the ground state is lowered in energy, and the first excited state shifts up. Therefore, the separation between these two states increases.

DOI: 10.1021/acsphotonics.5b00532
ACS Photonics 2016, 3, 249−254

Similar splitting in the energy spectrum can be seen in the higher energy states between 2.5−3.0 meV. The splitting is the Rabi-splitting.

Figure 4b shows TEC versus chemical potential at time t = 220 ps without a photon cavity g_γ = 0.0 meV (blue diamonds) and with a photon cavity for the electron−photon coupling strength g_γ = 0.05 (green squares), 0.10 (golden triangles), and 0.15 meV (red circles) in the case of resonant of the photon field. The temperature of the left lead is fixed at T_L = 1.16 K, implying thermal energy $k_B T_L$ = 0.10 meV, and the temperature of the right lead is assumed to be T_R = 0.58 K, with thermal energy $k_B T_R$ = 0.05 meV.

In the resonant photon field, a reduction in the TEC is observed with increasing electron−photon coupling strength. For g_γ = 0.05 meV, the following three states contribute to the electron transport at μ = 1.10 meV with "positive" current, and at μ = 1.40 meV with "negative" current: The ground state, the one-photon replica of the ground state and the first excited state. Increasing the electron−photon coupling strength to g_γ = 0.15 meV, the first excited state shifts up and does not participate in the electron transport. Therefore, the TEC is suppressed.

The TEC decreases at μ = 1.90 and 2.10 meV around the first excited state. The current suppression is due to participation of the one-photon replica of the first excited state with the energy 2.65 meV at g_γ = 0.05 meV. But at the higher electron−photon coupling strength g_γ = 0.15 meV, the one-photon replica of the first excited state is not active in the transport. This is because it moves up for high electron−photon coupling strength. Consequently, the TEC drops down. This reduction in the thermoelectric current is a direct consequence of the Rabi-splitting of the energy levels of the system. Earlier, we have established dynamic effects of the Rabi-splitting on the transport current through the system at a finite bias voltage.[37] The electrons are getting active in the transport around the second excited state. The activation of the electron transport there is due to the symmetry properties of the one-photon replica of the first excited state.

We have verified that the TEC flattens out as the temperature of both leads is increased, keeping their temperature difference constant.

Opposite to the off-resonant system, the initial photon number in the resonant system can change the TEC substantially, as is seen in Figure 5b. The reason is the larger separation between photon replica states here. Consequently, the place of the active photon replicas in the energy spectrum is important, and the initial photon number influences the TEC.

CONCLUSIONS

We studied numerically the thermoelectric transport properties of a short quantum wire interacting with either the off- or on-resonant cavity-photon field. The quantum wire is assumed to be connected to two electron reservoirs with different temperatures. The temperature gradient accelerates electrons from the leads to the quantum wire, creating a thermoelectric current.

We showed that a plateau in the TEC is formed due to symmetry properties of the energy states of the quantum wire and the leads in the case of no cavity photon field.

By applying a linearly polarized photon field, the photon replica states result in an inverted thermoelectric transport in the off-resonance regime. Moreover, in the on-resonant photon field the effects of a Rabi-splitting in the energy spectrum appears leading to a reduction in the thermoelectric current. In both regimes, the current plateaus that were formed in the absence of a photon field are removed due to the generation of photon replica states.

Our results point to new opportunities to experimentally control thermoelectric transport properties of nanodevices with a cavity photon field.

AUTHOR INFORMATION

Corresponding Authors

*E-mail: nzar.r.abdullah@gmail.com.

*E-mail: vidar@hi.is.

Notes

The authors declare no competing financial interest.

ACKNOWLEDGMENTS

Financial support is acknowledged from the Icelandic Research and Instruments Funds and the Research Fund of the University of Iceland. The calculations were carried out on the Nordic High Performance Computer Center in Iceland. We acknowledge the Nordic network NANOCONTROL, Project No. P-13053, and the Ministry of Science and Technology, Taiwan, through Contract No. MOST 103-2112-M-239-001-MY3.

REFERENCES

(1) Shakouri, A. Recent Developments in Semiconductor Thermoelectricity Physics and Materials. *Annu. Rev. Mater. Res.* **2011**, *41*, 399.

(2) Majumdar, A. Thermoelectricity in Semiconductor Nanostructure. *Science* **2004**, *303*, 777−778.

(3) Heremans, J. P.; Jovovic, V.; Toberer, E. S.; Saramat, A.; Kurosaki, K.; Charoenphakdee, A.; Yamanaka, S.; Snyder, G. J. Enhancement of Thermoelectric Efficiency in PbTe by Distortion of the Electronic Density of States. *Science* **2008**, *321*, 554−557.

(4) Hicks, L. D.; Dresselhaus, M. S. Effect of quantum-well structures on the thermoelectric figure of merit. *Phys. Rev. B: Condens. Matter Mater. Phys.* **1993**, *47*, 12727−12731.

(5) Saira, O.-P.; Meschke, M.; Giazotto, F.; Savin, A. M.; Möttönen, M.; Pekola, J. P. Heat Transistor: Demonstration of Gate-Controlled Electronic Refrigeration. *Phys. Rev. Lett.* **2007**, *99*, 027203.

(6) Beenakker, C. W. J.; Staring, A. A. M. Theory of the thermopower of a quantum dot. *Phys. Rev. B: Condens. Matter Mater. Phys.* **1992**, *46*, 9667−9676.

(7) Andreev, A. V.; Matveev, K. A. Coulomb Blockade Oscillations in the Thermopower of Open Quantum Dots. *Phys. Rev. Lett.* **2001**, *86*, 280−283.

(8) Svensson, S. F.; Persson, A. I.; Hoffmann, E. A.; Nakpathomkun, N.; Nilsson, H. A.; Xu, H. Q.; Samuelson, L.; Linke, H. Lineshape of the thermopower of quantum dots. *New J. Phys.* **2012**, *14*, 033041.

(9) Świrkowicz, R.; Wierzbicki, M.; Barnaś, J. Thermoelectric effects in transport through quantum dots attached to ferromagnetic leads with noncollinear magnetic moments. *Phys. Rev. B: Condens. Matter Mater. Phys.* **2009**, *80*, 195409.

(10) Juergens, S.; Haupt, F.; Moskalets, M.; Splettstoesser, J. Thermoelectric performance of a driven double quantum dot. *Phys. Rev. B: Condens. Matter Mater. Phys.* **2013**, *87*, 245423.

(11) Bagheri Tagani, M.; Rahimpour Soleimani, H. Thermoelectric effects through weakly coupled double quantum dots. *Phys. B* **2012**, *407*, 765−769.

(12) Broido, D. A.; Reinecke, T. L. Theory of thermoelectric power factor in quantum well and quantum wire superlattices. *Phys. Rev. B: Condens. Matter Mater. Phys.* **2001**, *64*, 045324.

(13) Vedernikov, M.; Uryupin, O.; Ivanov, Y.; Kumzerov, Y. Thermoelectric properties of semiconductor quantum wires. Proceedings of the 22nd International Conference on Thermoelectrics, ICT-2003, La Grande-Motte, France, August 17−21, 2003; pp 355−358.

DOI: 10.1021/acsphotonics.5b00532
ACS Photonics 2016, 3, 249−254

(14) Hochbaum, A. I.; Chen, R.; Delgado, R. D.; Liang, W.; Garnett, E. C.; Najarian, M.; Majumdar, A.; Yang, P. Enhanced thermoelectric performance of rough silicon nanowires. *Nature* **2008**, *451*, 163−167.
(15) Torfason, K.; Manolescu, A.; Erlingsson, S. I.; Gudmundsson, V. Thermoelectric current and Coulomb-blockade plateaus in a quantum dot. *Phys. E* **2013**, *53*, 178−185.
(16) Zimbovskaya, N. A. The effect of Coulomb interactions on thermoelectric properties of quantum dots. *J. Chem. Phys.* **2014**, *140*, 104706.
(17) Monteros, A.; Uppal, G.; McMillan, S.; Crisan, M.; Tifrea, I. Thermoelectric transport properties of a T-shaped double quantum dot system in the Coulomb blockade regime. *Eur. Phys. J. B* **2014**, *87*, n/a.
(18) Lim, J. S.; López, R.; Sánchez, D. Dynamic thermoelectric and heat transport in mesoscopic capacitors. *Phys. Rev. B: Condens. Matter Mater. Phys.* **2013**, *88*, 201304.
(19) Svensson, S. F.; Hoffmann, E. A.; Nakpathomkun, N.; Wu, P. M.; Xu, H. Q.; Nilsson, H. A.; Sánchez, D.; Kashcheyevs, V.; Linke, H. Nonlinear thermovoltage and thermocurrent in quantum dots. *New J. Phys.* **2013**, *15*, 105011.
(20) Sánchez, D.; Serra, L. m. c. Thermoelectric transport of mesoscopic conductors coupled to voltage and thermal probes. *Phys. Rev. B: Condens. Matter Mater. Phys.* **2011**, *84*, 201307.
(21) Tagani, M. B.; Soleimani, H. R. Thermoelectric effects in a double quantum dot system weakly coupled to ferromagnetic leads. *Solid State Commun.* **2012**, *152*, 914−918.
(22) Biele, R.; D'Agosta, R.; Rubio, A. Time-Dependent Thermal Transport Theory. *Phys. Rev. Lett.* **2015**, *115*, 056801.
(23) Chen, X.; Liu, D.; Duan, W.; Guo, H. Photon-assisted thermoelectric properties of noncollinear spin valves. *Phys. Rev. B: Condens. Matter Mater. Phys.* **2013**, *87*, 085427.
(24) Hochbaum, A. I.; Chen, R.; Delgado, R. D.; Liang, W.; Garnett, E. C.; Najarian, M.; Majumdar, A.; Yang, P. Enhanced thermoelectric performance of rough silicon nanowires. *Nature* **2008**, *451*, 163.
(25) Ojanen, T.; Jauho, A.-P. Mesoscopic Photon Heat Transistor. *Phys. Rev. Lett.* **2008**, *100*, 155902.
(26) Pascal, L. M. A.; Courtois, H.; Hekking, F. W. J. Circuit approach to photonic heat transport. *Phys. Rev. B: Condens. Matter Mater. Phys.* **2011**, *83*, 125113.
(27) Balachandran, V.; Bosisio, R.; Benenti, G. Validity of the Wiedemann-Franz law in small molecular wires. *Phys. Rev. B: Condens. Matter Mater. Phys.* **2012**, *86*, 035433.
(28) Abdullah, N. R.; Tang, C. S.; Manolescu, A.; Gudmundsson, V. Electron transport through a quantum dot assisted by cavity photons. *J. Phys.: Condens. Matter* **2013**, *25*, 465302.
(29) Gudmundsson, V.; Jonasson, O.; Tang, C.-S.; Goan, H.-S.; Manolescu, A. Time-dependent transport of electrons through a photon cavity. *Phys. Rev. B: Condens. Matter Mater. Phys.* **2012**, *85*, 075306.
(30) Jonasson, O.; Tang, C.-S.; Goan, H.-S.; Manolescu, A.; Gudmundsson, V. Nonperturbative approach to circuit quantum electrodynamics. *Phys. Rev. E* **2012**, *86*, 046701.
(31) Gudmundsson, V.; Jonasson, O.; Arnold, T.; Tang, C.-S.; Goan, H.-S.; Manolescu, A. Stepwise introduction of model complexity in a general master equation approach to time-dependent transport. *Fortschr. Phys.* **2013**, *61*, 305.
(32) Nakajima, S. On quantum theory of transport phenomena steady diffusion. *Prog. Theor. Phys.* **1958**, *20*, 948.
(33) Zwanzig, R. Ensemble Method in the Theory of Irreversibility. *J. Chem. Phys.* **1960**, *33*, 1338−1341.
(34) Gudmundsson, V.; Gainar, C.; Tang, C.-S.; Moldoveanu, V.; Manolecu, A. Time-dependent transport via the generalized master equation through a finit quantum wire with an embedded subsystem. *New J. Phys.* **2009**, *11*, 113007.
(35) Gudmundsson, V.; Lin, Y.-Y.; Tang, C.-S.; Moldoveanu, V.; Bardarson, J. H.; Manolescu, A. Transport through a quantum ring, dot, and barrier embedded in a nanowire in magnetic field. *Phys. Rev. B: Condens. Matter Mater. Phys.* **2005**, *71*, 235302.
(36) Moldoveanu, V.; Manolescu, A.; Gudmundsson, V. Geometrical effects and signal delay in time-dependent transport at the nanoscale. *New J. Phys.* **2009**, *11*, 073019.
(37) Gudmundsson, V.; Sitek, A.; Lin, P.-y.; Abdullah, N. R.; Tang, C.-S.; Manolescu, A. Coupled collective and Rabi oscillations triggered by electron transport through a photon cavity. *ACS Photonics* **2015**, *2*, 930.

DOI: 10.1021/acsphotonics.5b00532
ACS Photonics 2016, 3, 249−254